González Martínez, MC.; Tampau, A.; Chiralt, A. (2020). Poly(vinyl alcohol)-based materials encapsulating carvacrol obtained by solvent casting and electrospinning. Reactive and Functional Polymers. 153:1-10. https://doi.org/10.1016/j.reactfunctpolym.2020.104603

Polyvinyl alcohol-based materials encapsulating carvacrol obtained by solvent casting and electrospinning

Alina Tampau[*a]; Chelo González-Martínez[b]; Amparo Chiralt[c]

[a, b, c] Instituto Universitario de Ingeniería de Alimentos para el Desarrollo, Ciudad Politécnica de la Innovación, Universitat Politécnica de Valencia, Camino de Vera, s/n, 46022 Valencia, Spain.

[a] altam@upv.es, [b] cgonza@tal.upv.es, [c] dchiralt@tal.upv.es

Abstract

Carvacrol has been encapsulated in polyvinyl alcohol (PVA) matrices by electrospinning and casting. Aqueous solutions containing 15 % PVA and 15 % carvacrol with respect to polymer have been used, containing or not Tween 85 at 0.3 g/100 g carvacrol. Electrospun mats exhibited beads and thin fibres which became thinner and interrupted when carvacrol was present and retained up to 83 % of this compound. The encapsulation efficiency in the electrospun mats decreased in the presence of surfactant, reaching values similar to those of casting (75-77 %). The electrospun, surfactant free material was practically amorphous with 40 % of the total carvacrol non-thermally releasable. In contrast, when surfactant was present and in cast material, with 40 % crystallinity, the strongly bonded carvacrol ratio decreased. Specific PVA - phenolic hydroxyl interactions played an important role in the degree of carvacrol retention in the matrices, which depended on surfactant's presence and processing method.

Keywords: polyvinyl alcohol; carvacrol; electrospinning; casting; encapsulation efficiency.

1. Introduction

Nowadays, we are increasingly witnessing a higher consumer demand for safer foods. A modern strategy that provides an increase in food quality and safety is the use of "smart" active packaging that interacts with the food and its environment [1], [2]. These active packaging materials could control the permeability for gases and/or moisture, scavenge oxygen (to prevent foodstuff oxidation) or limit microbial growth, safely

[*]Corresponding author. E-mail address: altam@upv.es (Alina Tampau).

extending product shelf life. Also, the packaging industry is actively changing direction towards environmentally-friendly biodegradable components, stimulating the creation of new kinds of coatings and multilayer packaging materials for the food industry [1]. Nevertheless, currently the great majority of food-preserving packaging is based on oil-derived synthetic plastics, which, despite having multiple advantages (such as low cost, versatility, good barrier qualities), are not biodegradable, thus generating a significant environmental impact [3]. Then, the new packaging concept should be based on biodegradable materials in order to address these concerns.

Polyvinyl alcohol (PVA) is a synthetic polymer that is widely used for different applications in various branches of the industry, medicine and food sectors, obtained easily through the polymerization of vinyl acetate followed by the hydrolysis of the acetate groups [4]. It is water soluble, completely biodegradable, colourless and odourless, with good mechanical properties and biocompatibility. PVA also has the potential to act as a carrier matrix for the incorporation of active compounds [5].

Regarding the active compounds, natural substances could be used, such as plant extracts and essential oils, for the purposes of replacing the synthetic food preservatives. The essential oils (EO) are a complex blend of volatile and semi volatile substances, mostly made up of terpenes, terpenoids and aromatic compounds of low molecular weight. Different EO have proven to exhibit antimicrobial properties against bacteria [6], [7], or fungi [8], and have been recognized as safe compounds (GRAS) to be used in the food industry by legal organisms, such as the Food and Drug Administration in the USA. Nevertheless, despite their advantages, the concentration levels of EO that would exert the desired effects could also introduce unwanted flavours and potential fitotoxicity into the foodstuffs they are required to protect. This is the case of carvacrol (CA), a monoterpenoid phenol that can be found in high concentrations in the EO of oregano or thyme [9], with proven antimicrobial and antioxidant effects. It is considered a good preservative for a wide range of foodstuffs [10], but its direct application is limited because of its strong flavour, high volatility, low water solubility or its potential reactions with certain food components that might alter the food properties and limit its efficacy as a preservative [11], [12]. The encapsulation of the active compounds may favour their stability, their preservation efficiency while allowing for a controlled release towards the foodstuffs [13].

One encapsulation method that is gaining interest in the food packaging sector is the electrospinning (ES) technique [14], [15]. It has a simple working principle, using an electric field to stretch a polymeric solution, forming structures (mainly fibres) with high specific surface that can be used to coat support materials useful in the development of multilayer active packaging [16]. Some successful applications have been reported, such as antioxidant multilayers constituted by polylactide (PLA) cast films coated by ES with PLA mats encapsulating gallic acid [17], antimicrobial multilayer systems composed of a polyhydroxyalkanoate (PHA) support coated with an electrospun layer of PHA enriched with silver nanoparticles [18], and antibacterial multilayers with reduced water barrier properties developed from gelatine sheets coated by ES with poly-ε-caprolactone loaded with black pepper oleoresin [19].

In the development of active multilayer materials, the extension of a polymer solution containing the active compound on a polymeric support can also be used to obtain coated films with an active layer, where the active compound would be encapsulated into the polymer matrix of the cast layer. However, the effective extension of a determined active-polymer solution will be greatly affected by the solutions' wettability and spreadability on the supporting polymer layer, which in turn, depend on the contact angle of the polymer-solution system and surface tension of the solutions. All these factors play a crucial role in the coating thickness and effectiveness. Additionally, the concept of multilayer films involves the assembly of polar and non-polar polymers to take advantage of their respective complementary barrier properties to gases and water vapour. In this sense, the effective extension of polymer polar solutions on non-polar polymers or vice versa has the problems associated with the lack of chemical affinity. In contrast, the ES technique allows for the electrodeposition of the solvent-free polymer on the supporting film surface, thus avoiding the problems of the extension of the solution.

The electrodeposition of polyvinyl alcohol has been studied by several authors. [20] and [21] studied the influence of different parameters, such as molecular weight and concentration on the ES process. The electrospun fibre architecture depended on the PVA molecular weight (M_w) and its concentration in the solution; beads and spindle-like formations being more present at lower concentrations or lower M_w than fibres. The diameter of fibres became larger as M_w or concentration increased, and a broader fibre distribution could be obtained. The presence of salts (such as NaCl) in the solution could disrupt the fibrous assembly for a low M_w polymer, however for the

higher M_w the salt presence leads to thinner fibre diameters. The formation of PVA fibres was not affected by the pH variation, but an increase in voltage and salt concentration was not favourable to the ES process [21]. [14] reviewed the use of the electrospun PVA matrix as a carrier for different active substrates, such as silver particles, medicinal drugs, enzymes, bifidobacteria, or plant essential oils. [13] successfully obtained electrospun PVA nano-mats with uniform fibres containing cinnamon essential oil entrapped in β-cyclodextrin. The authors demonstrated that the ES process is favourable to maintaining the volatile active compound in the electrodeposited mat, which also presents thermal stability, due to the molecular interactions between the PVA, the essential oil and the β-cyclodextrin.

The purpose of this study was to analyse the ability of PVA to encapsulate carvacrol, incorporating or not surfactant, by means of the ES technique, in comparison with the casting method. The characterisation of the obtained materials in terms of the encapsulation efficiency, microstructure and thermal behaviour was carried out.

2. Materials and methods

2.1.Materials and reagents

Polyvinyl alcohol (PVA) (Mw 13,000-23,000; 87-89 % hydrolyzed), polyoxyethylene sorbitan trioleate Tween 85 (T85), carvacrol (CA) and phosphorous pentoxide (P_2O_5) were acquired from Sigma-Aldrich (Sigma–Aldrich Chemie, Steinheim, Germany). Purified water (resistivity of 18.2 MΩ cm) was prepared using a MilliQ Advantage A10 equipment from Millipore S.A.S., Molsheim, France. Absolute ethanol (UV grade) used for extraction was obtained from Panreac AppliChem (Panreac Química S.L.U, Barcelona, Spain).

2.2.Preparation of the liquid formulations

Aqueous solutions of PVA (15 wt. %) were prepared by dissolving the polymer in milli-Q water, under constant stirring at 80 ºC, for one hour. This concentration was selected on the basis of preliminary trials using 12.5, 15 and 20 % of PVA, in which 15 % wt. of PVA imparted the proper viscosity to the ES processing. CA was added in a ratio of 15 % (w/w) with respect to the PVA content. Formulations were prepared with and without surfactant (S), using a wt. ratio of 0.3:100 S:CA. This ratio was estimated on the basis of an expected CA droplet diameter of about 10 μm and considering an

excess surface concentration for the surfactant of 5 mg/m^2, in the range of the previously reported values [22]. The blend was mixed at 12,000 rpm for 3 minutes, using an Ultra Turrax rotor–stator homogenizer (Model T25D, IKA Germany). Control solutions with pure PVA were also prepared.

All the formulations were allowed to rest at room temperature for 24 h post-preparation, to assess their stability and promote the natural degassing process and, afterwards, these were degassed under vacuum. All the dispersions showed good stability without phase separation. Each liquid formulation was processed either by electrospinning (ES) or casting to obtain fibres or films, respectively, with entrapped carvacrol. The obtained materials were labelled as P for PVA, C for carvacrol and S for surfactant, preceded by C (casting) or ES (electrospinning), according to the processing method.

2.3.Obtaining the dry encapsulating material

To obtain the electrospun materials, the liquid formulations were loaded onto Fluidnatek **electrospinning** equipment (Bioinicia, Valencia, Spain) presenting the same setup as described by Tampau et al. (2017). The emulsions were fed through a BD luer-lock syringe (BD, Franklin Lakes, NJ, USA) at a flow rate varying between 0.25 and 0.5 mL/h, and a voltage in the range of 20-25 kV was applied. The collector plate was positioned 15 cm from the injector needle. All the applications were performed under room temperature conditions (25 ºC and 45 % RH). The obtained material was placed in a desiccator with P_2O_5 to avoid moisture absorption till further analysis.

To obtain the **cast** films, an equivalent of 1.5 g of PVA/plate of the aqueous formulations was poured onto levelled Teflon plates of 15 cm in diameter and dried at 25 ºC and 45 % RH for 48 h. The resulting dry films were peeled off and stored in a desiccator with P_2O_5 till further analysis.

2.4. Characterization of the liquid systems

2.4.1. Particle size distribution

The droplet size of the emulsions was evaluated using the laser diffractometer MasterSizer 2000 (Malvern Instruments, Worcestershire, UK) in order to assess their particle size distribution. Each formulation was dispersed in distilled water at 1000 rpm

(to avoid formation of bubbles) until an obscuration range of 5 % was reached. The size distribution graphs were obtained.

2.4.2. Rheological behaviour

The rheological behaviour of the PVA-based formulations was assessed in triplicate by means of a rotational rheometer (HAAKE Rheostress 1, Thermo Electric Corporation, Karlsruhe, Germany) with a system of coaxial cylinders type Z34DIN Ti. The samples were stabilized for 15 minutes at 25 ºC after being poured into the coaxial cylinder. The shear stress (σ) was measured as a function of shear rate ($\dot{\gamma}$) from 0 to 100 s^{-1}, allowing the equipment a 5 min ramp-up (to reach the maximum shear rate) and a 5 min ramp-down (to return to zero shear rate). The power law model (**eq. 1**) was used to determine the flow behaviour index (n) and the consistency index (K). The viscosity at near zero shear rate (η_0) was determined from the initial slope of the flow curves.

$$\sigma = K \cdot \dot{\gamma}^{n} \qquad \text{[eq. 1]}$$

2.4.3. Conductivity, surface tension and ζ potential

The **conductivity** of the emulsions was analysed by means of a conductimeter (model SevenEasy, Mettler Toledo, Schwerzenbach, Switzerland). Each formulation was measured in triplicate, after being diluted 1:100 (v/v) with milli-Q water.

The **surface tension** was determined using the pendant drop method, with OCA 20 equipment (Dataphysics, Germany) and the measurements were processed by SCA 20 software package. For each formulation, 20 measurements were performed.

Finally, the **ζ-potential** was assessed in triplicate in the diluted emulsions (1:100 (v/v)), using DTS1070 cuvettes and Zeta Sizer nano series equipment (Malvern Instruments, Worcestershire, UK). The electrophoretic mobility registered by the equipment was converted into **ζ-potential** by applying the Smoluchowsky model [23].

2.5. Characterization of the solid material

2.5.1. Microstructure

The microstructure of the obtained materials was analysed by using Field Emission Scanning Electron Microscopy (FESEM Ultra 55, Zeiss, Oxford Instruments, UK). The

cast films were cryo-fractured by immersion in liquid nitrogen (to allow for cross-section view), while the electrospun material was deposited over an aluminium foil support surface and observed directly. The samples were mounted on stubs with carbon tape, and after platinum sputtering in an EM MED020 (Leica Microsystems, Germany), were observed using an accelerating voltage of 1 kV.

2.5.2. Encapsulation efficiency

The CA retention in the films and in the electrospun material was quantified by using a UV/Vis spectrophotometer (Evolution 201 UV-Vis, Thermo Fisher Scientific Inc.), using quartz cuvettes, as described by Tampau et al. (2017). Briefly, samples of up to 30 mg of dry material were placed in amber vials along with 15 mL of absolute ethanol, and after being hermetically sealed, were maintained under stirring for 24 h at room temperature. The alcoholic extracts were analysed at 275 nm, using the extract of the CA-free matrix as blank. The absorbance data were converted into concentration units by using a calibration curve (concentration=66.643 x Abs, R^2=0.999), obtained previously from the absorbance measurements of standard carvacrol solutions (between 4-100 µg CA/mL). The encapsulating efficiency (EE) was expressed as a percentage, representing the quotient between the CA alcohol-extracted in the films and the theoretical CA content. This analysis was performed in triplicate for each formulation.

2.5.3. Thermogravimetric analysis (TGA) and differential scanning calorimetry (DSC)

The obtained films and ES material were submitted to thermal analyses, in order to characterize their thermal degradation (TGA) and assess the carvacrol effect on the thermal behaviour of the polymer by differential scanning calorimetry (DSC). For the TGA assay, the previously conditioned samples (10 mg) were placed in 70 µL alumina crucibles in a thermo-gravimetric analyser (TGA/SDTA 851e, Mettler Toledo, Schwarzenbach, Switzerland) and heated from 25 to 700 ºC at a rate of 10K/min, under a nitrogen flow (20 mL/min) to avoid oxidative processes. The DTA curves were obtained and the onset, peak and endset temperatures of the degradation peaks were determined, as well as the percentage of weight loss for each of them. The differential scanning calorimetry analysis was carried out in DSC (1 StarE System, Mettler-Toledo, Inc., Switzerland) equipment. Samples (5-10 mg) of the previously P_2O_5 conditioned

films or fibres were placed into aluminium pans (Seiko Instruments, P/N SSC000C008) and tightly sealed. The samples were first kept at -25 ºC for 5 minutes and then heated at a rate of 10 K/min from -25 to 225 ºC, where they were maintained for 5 minutes. Then a cooling step was applied from 225 to -25 ºC, at the same cooling rate. After being kept at -25 ºC for 5 minutes, a second heating step followed, going from -25 to 250 ºC, at 10 K/min. As reference, an empty aluminium pan was used. The weight fraction of crystalline regions (X_c: crystallinity index) was calculated from both heating steps, comparing the obtained enthalpy to the fusion enthalpy of 100 % crystalline PVA (ΔH=138.6 J/g, [24]). Each sample was analysed in triplicate.

2.6. Statistical analysis

The analysis of the data was performed through variance analysis (ANOVA) using the Statgraphics Centurion XVII.64 software. To discern between formulations, the Fisher Least Significant Difference (LSD) ($p<0.05$) was used. DSC data were also analysed using a multifactor analysis of variance with 95 % significance level, considering as factors: type of formulation (P, PC, PCS) and processing method (C or ES).

3. Results and discussion

3.1. Properties of the liquid systems

Rheological behaviour, conductivity, surface tension and the emulsion droplet size (in the case of systems containing CA) of the liquid systems can affect their behaviour in ES processing as well as the microstructure of the electrospun material. So, these parameters were characterised in order to better understand differences between samples.

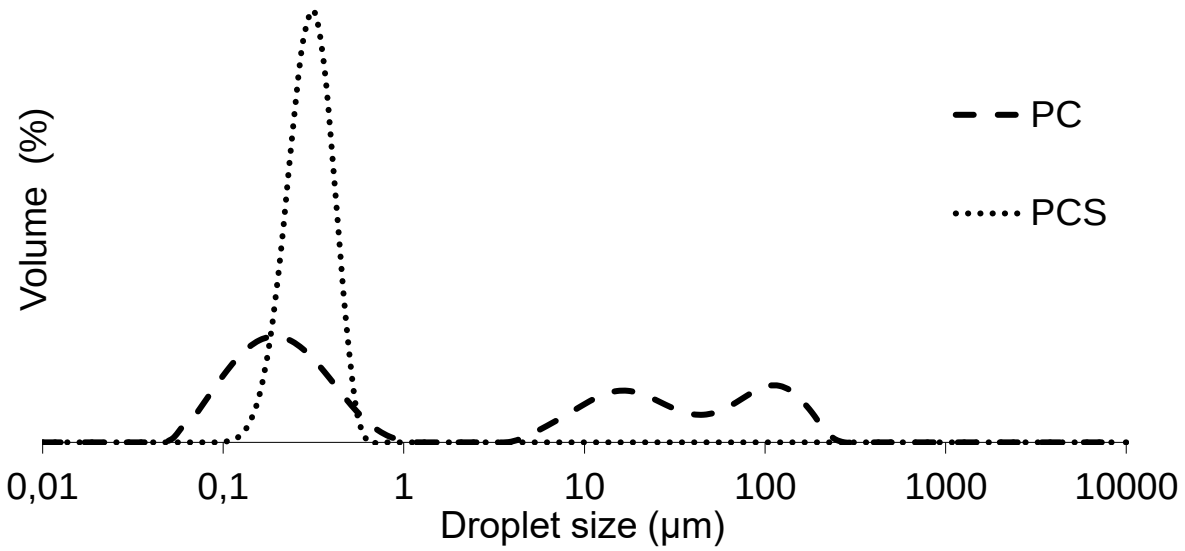

Figure 1. Typical particle size distribution of the different emulsions containing carvacrol.

Figure 1 shows the droplet size distribution of the emulsions containing carvacrol with and without surfactant. The presence of the surfactant gave rise to a unimodal particle size distribution, with smaller droplet diameters (under 1 µm), in agreement with the formation of small T85 micelle-entrapping CA. The particle size was lower than that expected from the surfactant-CA ratio used, which suggests that only a part of the incorporated carvacrol was inside the micelles. When no surfactant was added, the particle size distribution turned multimodal. This suggests the formation of aggregates of CA droplets through flocculation and coalescence processes, or even chain-droplet aggregations promoted by the CA interactions with the polymer. Specific CA-polymer interactions could be deduced from the sharp increase in the liquid phase viscosity when CA was incorporated into the PVA solution. **Figure 2** shows the flow curves of the three aqueous formulations (P, PC and PCS) where the Newtonian flow of the PVA solution turned pseudoplastic when CA was incorporated for both surfactant-free liquid (PC) and that containing surfactant (PCS).

Formulation	η_0 (Pa·s)	n	k
P	0.07±0.00[a]	1.004±0.002[c]	-
PC	14.23±0.53[c]	0.716±0.004[a]	6.08±0.16[b]
PCS	11.65±0.13[b]	0.733±0.001[b]	5.23±0.04[a]

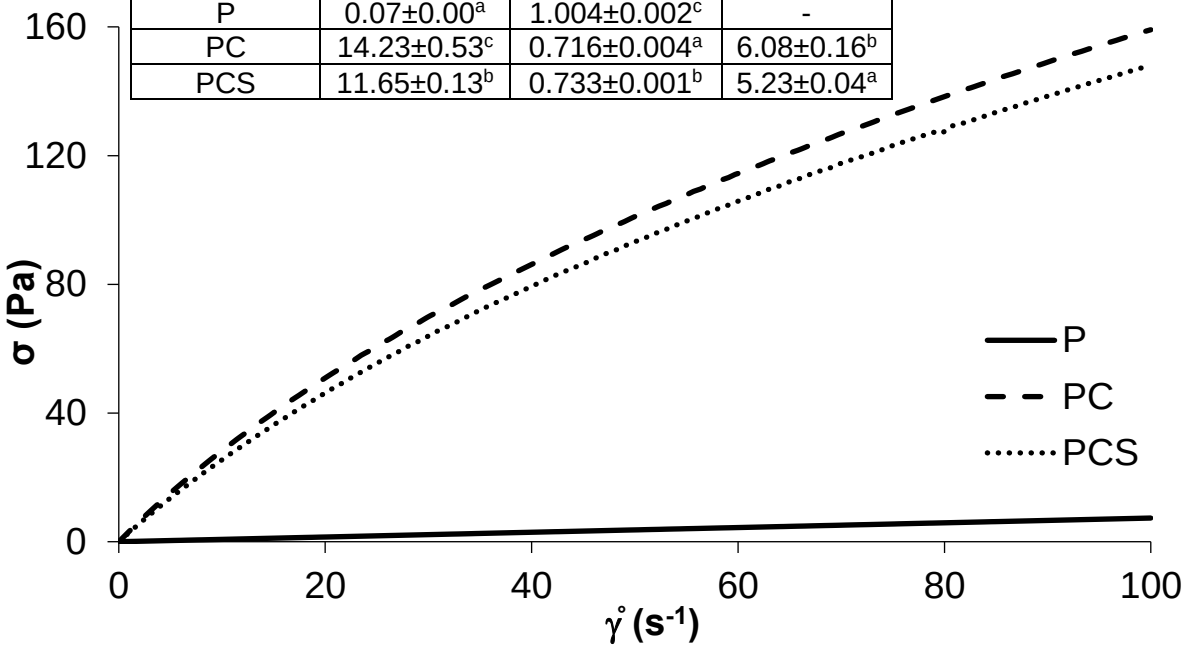

Figure 2. Rheological curves of the different PVA-based emulsions. Apparent viscosity η_0 (Pa·s) at a near zero shear rate $\dot{\gamma}$ (initial slope of the flow curves), flow behavior index (n) and consistency index (K) are also presented, with mean values and standard deviation.

The volume fraction of the dispersed phase was about 2.3 % in both cases whereas the viscosity at near zero shear rate increased approximately 200 or 165 times (**Figure 2**), respectively for the surfactant-free emulsion and that containing surfactant. This marked rise in viscosity suggests specific interactions of CA with the polymer. In fact, acetylated groups of PVA chains can be ionized, exhibiting negative charge, according to the mechanism described by [25], which could promote the binding with the CA phenolic hydroxyl group, which can act as a Lewis electron acceptor, thus being bonded to the polymer chain, forming Lewis adducts. These interactions could lead to an increase in the liquid viscosity when CA is incorporated, additionally to the effect of the dispersed phase concentration, since the hydrodynamic volume and intrinsic viscosity of PVA chains will increase by bonding the carvacrol molecules. When surfactant is present, the CA entrapment in the T85 micelles could limit the CA bonding to the PVA chains while the smaller droplet size in the emulsion may also contribute to the reduction in viscosity.

Table 1. Conductivity (κ), surface tension (γ) and ζ-potential of the emulsions, diluted or not in milli-Q water. Average values and standard deviations. Different superscript letters in the same column indicate significant differences ($p<0.05$) between samples.

Formulation	κ (μS/cm)	γ (mN/m)	ζ-potential (mV)
	dilution 1:100 (v/v)	without dilution	dilution 1:100 (v/v)
P	28.9±0.1[b]	42.2 ± 0.7[b]	-13±3[a]
PC	21.5±0.4[a]	31.5 ± 0.4[a]	-7±2[b]
PCS	44.5±0.1[c]	31.3 ± 0.3[a]	-11.6±0.6[a]

They reported that with an increase in solution viscosity, both beaded fibre and the bead diameter increased while the density of beads decreased: NO SE CUMPLE
The greater viscosities the bead shape became less spherical and more spindle-like, resulting in nanofiber formation with diminished bead defects. A high surface tension of the solution at lower levels of polymer concentration caused the fiber jet to fragment into droplets. Viscoelastic forces competed with the surface tension in the nanofiber jet and an increase in viscosity therefore favored the formation of smooth nanofibers.
Generally it has been observed that an increase in solution conductivity results in a substantial decrease in nanofiber diameter: NO SE CUMPLE
However, the viscosities in the upper range resulted in incomplete drying of the polymer nanofiber thereby influencing the morphology of the formed nanofibers.

The solution film forming physicochemical properties, such as conductivity, surface tension and viscosity usually affect the performance of the fabricated nanofibers. In general, an increase in viscosity caused an increment in both the bead and bead fibre diameter while density of beads decreased. On the other hand, an increase in solution conductivity resulted in a substantial decrease in nanofiber diameter (Pillay et al, 2013).
In our experiments, the relatively high surface tension of the solutions caused the fiber jet to fragment into droplets in all cases, leading to the appearance of bead-fibre structures. Furthermore, no effect of the viscosity was observed in the dispersions with the greater viscosity (PC, PCS), which showed thinner fibre diameters than the pure P solution. This can be explained taking into account their surely due to the increment in the conductivity which has an opposite effect on the fibre diameter size.

The obtained values for conductivity, surface tension and ζ-potential of the liquid systems are shown in **Table 1**. Conductivity decreased in the liquid systems when CA was incorporated and increased when surfactant was present. Differences in the sample conductivity revealed a different surface charge density in the polymer chains or droplets. The PCS system exhibited the highest conductivity values, followed by the pure PVA formulation. The incorporation of CA decreased the conductivity values, probably due to the combination between the neutralizing effect upon acetate groups and the formation of aggregates with lower mobility, as revealed by the particle size distribution curve. The higher conductivity values registered for the PCS emulsion can be explained by the different interactions taking place in the presence of the surfactant, which lead to the formation of smaller particles, decreasing the viscosity and limiting CA-PVA interactions. Coherently with the changes in conductivity, the negative ζ-potential values of pure PVA associated with the ionization equilibrium decreased

when the system contained CA, in agreement with the described mechanism shown in **Figure 3**. According to the acetylation degree of the chains, the molar ratio of the incorporated carvacrol and acetylated groups was estimated to be 1:3, which implies that there were not enough carvacrol molecules in the system to react with all the negative charges of the chains, in agreement with the negative zeta potential value obtained for the PC system. In emulsions containing surfactant, the smaller reduction in zeta potential is coherent with the fact that a part of the carvacrol molecules is entrapped in the core of the surfactant micelles. Then, a partition of carvacrol between the Lewis adducts in the polymer chains and T85 micelles seems to occur.

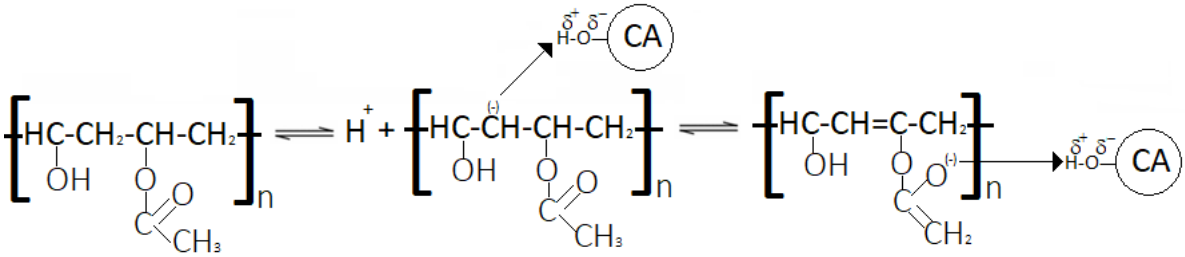

Figure 3. Ionization mechanism of the acetate group within the PVA polymer chain, according to [25] and proposed mechanism for PVA-carvacrol interactions.

As concerns the surface tension (ST) (**Table 1**), all PVA formulations presented ST values lower than the solvent (72 $mN \cdot m^{-1}$) and in the range of that previously determined by other authors [26]. Because of the presence of -OH groups, PVA has the capability of H-bonding with the solvent, exhibiting a tendency to migrate from bulk to the surface, thus decreasing its surface tension, like other surface-active agents [26]. The presence of carvacrol, with and without surfactant enhanced this surfactant effect, and lower values of surface tensions were obtained for these liquid systems. The changes in the chain hydrophobicity associated with the binding of carvacrol could explain this effect, due to the promotion of the polymer adsorption at the air-liquid interface. Likewise, the presence of droplets or micelles at the air-liquid interface will also reduce the liquid surface tension. The addition of the T85 did not significantly modify the ST value with respect to the PC system, probably due to its prevalent location at the water-carvacrol interface in the micelles. Relatively low values of surface tension favour the ES process, given that the electrostatic forces induced by the electric field must overcome the surface tension of the liquid.

It is remarkable that the obtained emulsions did not exhibit creaming or phase separation throughout more than 2 weeks and were considered stable and able to be processed by ES or casting.

3.2.Characterization of the solid material

The FESEM micrographs obtained for the cast and ES material are shown in **Figure 4**.

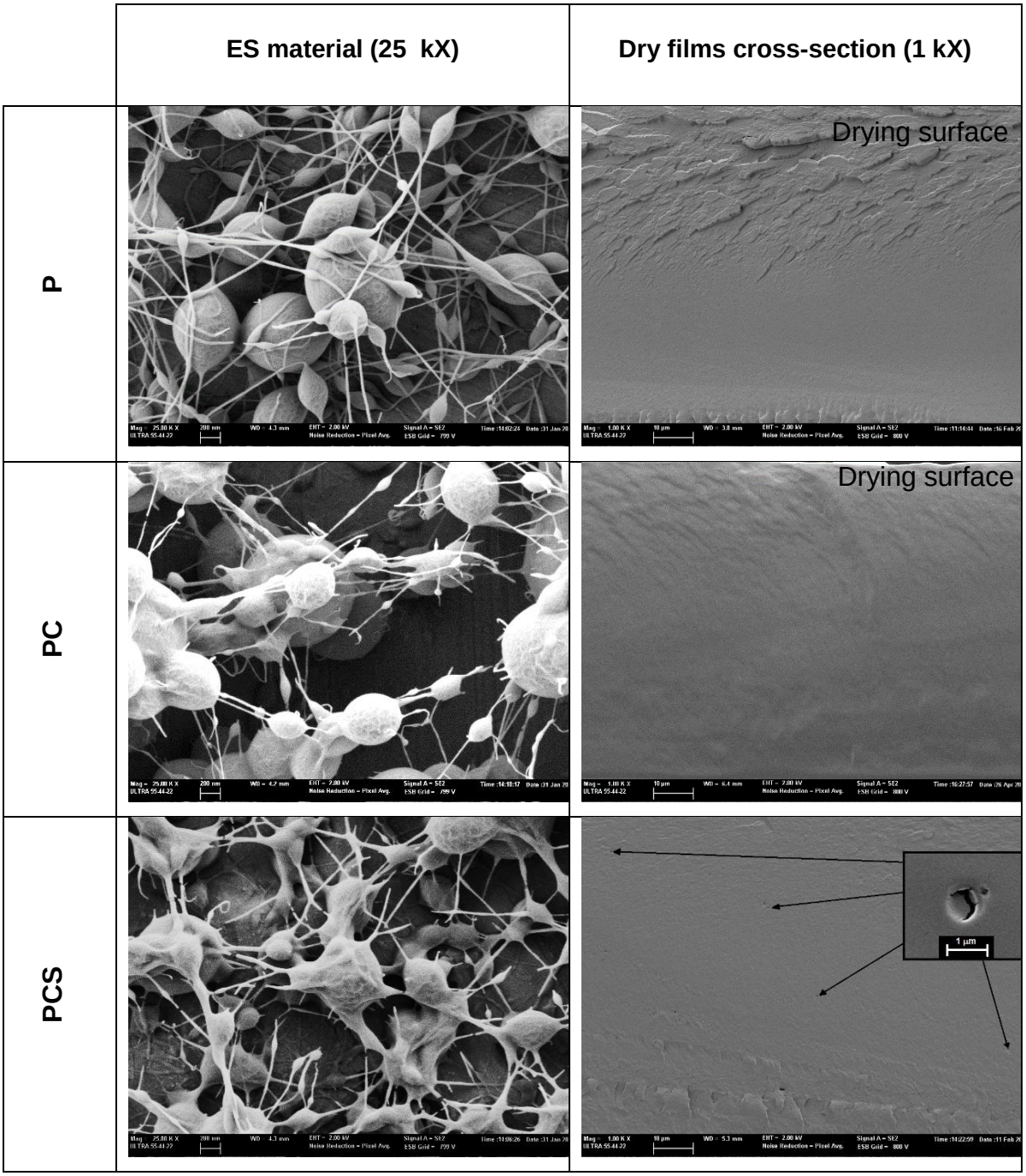

Figure 4. FESEM micrographs of the different ES materials and cross section of the PVA films. Higher magnification of small particles in the C-PCS sample was included.

It can be observed that the electrodeposition of the polymeric emulsions generated mostly thin fibres and spherical structures, with a few spindle-like shapes. Spherical formations could be mainly due to the low molecular weight of the polymer, reported by other authors [20], [27]. The presence of CA with and without T85 gave rise to thinner and less continuous fibres. This could be attributed to the previously commented on interactions of CA and PVA chains, which could modify the chain interactions under the electric field. Weak interactions could lead to thinner and more brittle fibres, which appear interrupted and that also break easily under the electron field during microscopy observations. Fibre formation was also limited in other emulsified systems [16]. In all cases, the specific surface generated through electrodeposition was large, providing a potentially wide surface for the active to be released.

The cross-sections of the cast films showed a fairly homogenous structure, without visible droplets of carvacrol when no surfactant was used, which suggested a complete integration of the active into the polymeric matrix through the aforementioned interactions between CA and PVA chains. Nevertheless, the PCS micrograph presented small spherical particles distributed in the matrix, which can be assigned to the preserved T85-Carvacrol micelles. These can be more clearly observed at higher magnification.

Table 2. Carvacrol encapsulating efficiency (EE) and content determined in the ES and cast samples. Average values and standard deviations.

Formulation	EE (%)	g CA/ 100 g PVA	g CA/ 100 g fibre or film
ES-PC	83 ± 9^{b}	12±2^{b}	11±1^{b}
ES-PCS	77 ± 7^{ab}	11±1^{ab}	10±1^{ab}
C-PC	75 ± 2^{a}	10.9±0.3^{a}	9.8±0.2^{a}
C-PCS	76 ± 3^{ab}	11.0±0.4^{ab}	9.9±0.3^{ab}

^{a,b,c} Different superscript letters in the same column indicate significant differences ($p<0.05$) between samples.

The encapsulating efficiency (EE) determined by extraction with absolute ethanol for ES and cast materials is shown in **Table 2**. Given the aqueous nature of the solvent and the formation of immiscible blends with carvacrol, the losses of the active during water evaporation by steam drag effect can be expected in both processing methods, according to previous studies [16], [28]. Nevertheless, CA-loaded samples exhibited

high retention degree, with an encapsulation efficiency of about 80 % and 75 % for ES and cast materials, respectively. This could be attributed to the high viscosity of the liquid medium, which limited the emulsion destabilization during the solvent evaporation, as well as to the described specific CA-PVA interactions, which helped to efficiently retain CA molecules inside the fibres or film structure. No significant differences in the EE values were obtained when incorporating T85, which indicated that the surfactant did not contribute efficiently to improving the emulsion stability during the solvent evaporation period. When carvacrol was encapsulated by using the ES process, the retention values were higher than when encapsulated by casting, although this difference was only significant ($p<0.05$) for the T85-free formulation. This is coherent with the fact that the addition of T85 limited the CA binding to the PVA chains, as previously commented on. The bonded carvacrol would be less sensitive to evaporation by steam drag effect than the carvacrol in micelles, which are sensitive to destabilization mechanisms releasing carvacrol. Then, higher EE values would be obtained in the absence of surfactant, especially when a fast water evaporation occurred in the electrospinning process.

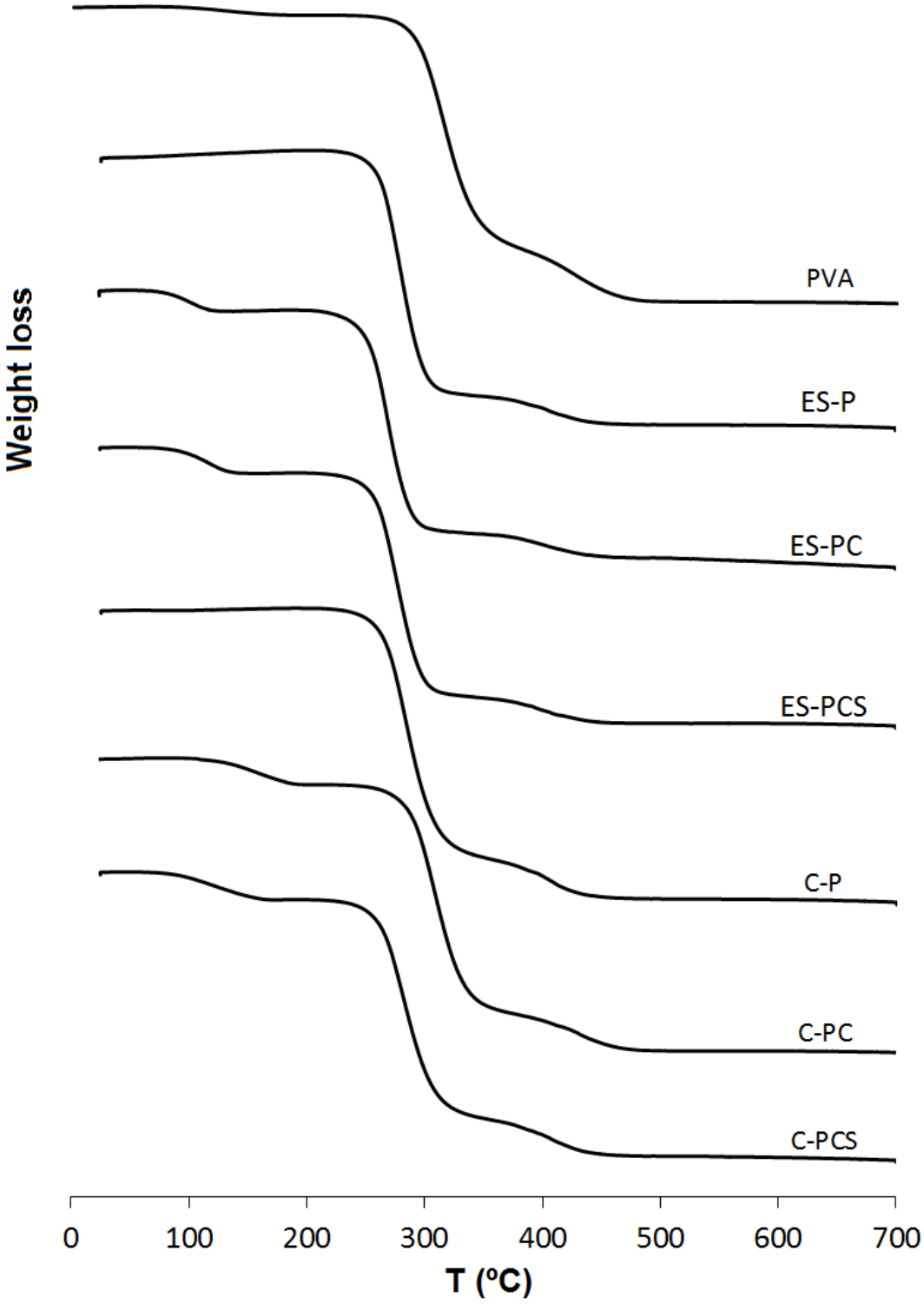
Weight loss
PVA
ES-P
ES-PC
ES-PCS
C-P
C-PC
C-PCS
0
100
200
300
400
500
600
700
T (ºC)

394

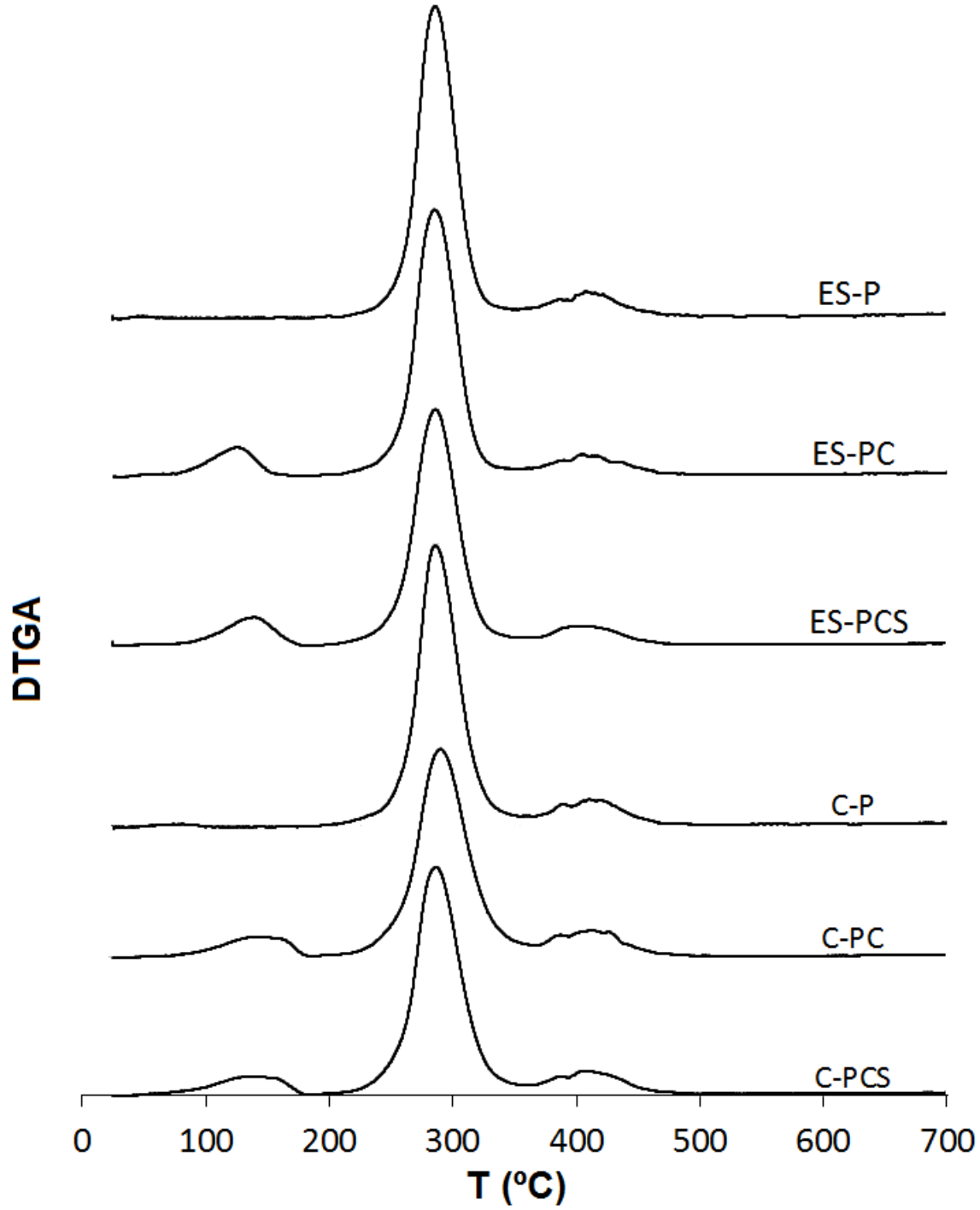

Figure 5. TGA and DTGA thermograms of the electrospun (ES) and cast (C) samples.

As concerns the thermal stability of the materials, **Figure 5** shows the weight loss and derivative (DTGA) curves for the different material formulations, together with that obtained for the pure components. Likewise, the temperatures for the different degradation steps of the samples are summarized in **Table 3**. For PVA films, two weight loss steps were observed: the first step between 200-300 ºC, in which the dehydration, chain scission and decomposition of the polymer take place and the

second step, around 400 ºC related with the degradation of the by-products generated by PVA during the thermal process [29]. Losses of adsorbed or bound water were not detected as the samples were previously conditioned with P_2O_5. All CA-added formulations presented a first weight loss step, starting at around 50 ºC, which could be attributed to the thermo-released fraction of the active (**Figure 5**), which showed the peak temperature between 109 and 135 ºC, depending on the sample. For cast films, the thermo-liberation of CA exhibited a similar pattern with a sustained release up to about 150 ºC, whereas the ES samples showed a thermo-release of CA a lower temperature (peaks: 121 and 109 ºC respectively for samples with and without surfactant). In contrast, by comparing the amounts of thermo-released CA (**Table 3**) with the determined content in the samples (**Table 2**), a strongly bonded fraction of this component to the polymer matrix could be deduced, since the total content was not thermo-released before the polymer degradation. This strongly bonded fraction represented 18 % of the total CA for cast films, regardless of the presence of surfactant, and 40 and 1 %, for ES samples without and with surfactant, respectively. These results indicate that CA was more strongly bonded to PVA in ES samples when no surfactant was added and the presence of surfactant did not affect the CA bonding degree in cast films. The thermo-release of CA at lower temperature in ES samples must be related with the greater specific surface area of the ES material, which facilitates the fast release of the compound. As previously commented on, the presence of surfactant limited the bonding of carvacrol to the polymer chains by the formation of the CA-surfactant micelles, which, as previously commented on, represent a weaker bonding of the compound within the polymer matrix. However, this effect was less remarkable in cast films where the longer drying times allow for the establishment of a structure nearer the equilibrium state (minimum free energy) where the components are arranged according to the more favourable interactions (affinity), with a higher CA ratio bonded to the PVA chains.

Table 3. Degradation temperatures (onset-T_o and peak-T_p) of **A**) individual components of the emulsions and **B**) the dry materials obtained by electrospinning and casting. Thermo-released CA fraction referred per 100 g polymer is also shown. Different superscript letters in the same column indicate significant differences ($p<0.05$) between samples.

A	**Component**	**T_o (ºC)**	**T_p (ºC)**

Carvacrol	77±6[a]	159±7[a]
PVA	197±2[b]	293±5[b]
Tween 85	335±2[c]	380±2[c]

435

B

Formulation	1st peak CA release		Thermo-released CA fraction	2nd peak PVA main degradation		3er peak by-product degradation	
	T_o (ºC)	T_p (ºC)	(g/100 g PVA)	T_o (ºC)	T_p (ºC)	T_o (ºC)	T_p (ºC)
ES-P	-	-	-	190±3[ab]	281±2[b]	394±10[a]	394±10[a]
ES-PC	48±1[a]	109±7[a]	7±1[a]	187±4[a]	275±6[a]	402±8[a]	406±6[b]
ES-PCS	46±3[a]	121±8[b]	10±1[b]	189±1[ab]	279±3[ab]	395±3[a]	395±3[a]
C-P	-	-	-	192±1[b]	288±4[c]	391±12[a]	399±6[ab]
C-PC	44.8±0.4[a]	135±3[c]	9±1[b]	191±1[b]	289±2[c]	397±4[a]	397±4[ab]
C-PCS	47±3[a]	129±4[bc]	8.9±0.2[b]	191±2[b]	287±3[c]	393±5[a]	393±5[a]

436 As regards the degradation temperature of PVA, the values were significantly affected
437 ($p<0.05$) by the film processing method. Thus, the thermogravimetric analysis revealed
438 that the degradation temperature (T_p) was significantly lower ($p<0.05$) in electrospun
439 PVA films than in those obtained by casting. These differences could be attributed to
440 the differing degree of polymer crystallization in each case, as crystallinity influences
441 many polymer properties, including mechanical and thermal. In this sense, a lower
442 crystallinity degree usually implies lower degradation temperatures [30]. Most
443 electrospun fibres exhibit a lower crystalline structure due to fast water evaporation
444 and polymer solidification during the electrospinning process [31], [32], as deduced
445 from the DSC analysis commented on below, which could explain their lower thermal
446 stability. Neither the presence of carvacrol nor T85 caused any significant differences
447 in the degradation temperature of the polymer for samples obtained using the same
448 processing method.

449 **Table 4**. DSC parameters of the PVA phase transitions: enthalpies (ΔH), crystallinity
450 index (X_c), melting (T_m), crystallization (T_c) and glass transition (T_g) temperatures
451 obtained in the different heating and cooling scans. Different superscript letters in the
452 same row indicate significant differences ($p<0.05$) between samples.

	ES-P	ES-PC	ES-PCS	C-P	C-PC	C-PCS

1st heating	ΔH_m (J/g PVA)	-	-	-	50±3^{a}	54±13^{a}	55±10^{a}
	X_C (%)	-	-	-	36±2^{a}	39±10^{a}	40±7^{a}
	T_m peak (ºC)	196±4^{a}*	180±4^{a}*	174±31^{a}*	186±3^{a}	186±3^{a}	189±3^{a}
	T_g (ºC)	37±3^{abc}*	31±2^{a}*	33±5^{a}*	55±2^{d}	41±8^{bc}	42±1^{c}
Cooling step	ΔH_c (J/g PVA)	24±4^{a}	30±3^{a}	25±6^{a}	29±2^{a}	26±5^{a}	22±6^{a}
	T_c onset (ºC)	156±9^{a}	168±1^{b}	166±6^{ab}	164±1^{ab}	169±6^{b}	158±8^{ab}
	T_c peak (ºC)	142±12^{a}	157.0±0.4^{a}	144±22^{a}	152±1^{a}	156±7^{a}	145±12^{a}
	T_g (ºC)	62±1^{c}	43±3^{a}	56±3^{b}	60±2^{c}	49±6^{a}	56±5^{b}
2nd heating	ΔH_m (J/g PVA)	26±7^{a}	39±2^{c}	28±4^{ab}	35±1^{bc}	29±5^{ab}	23±5^{a}
	X_C (%)	22±3^{abc}	29±2^{d}	24±3^{bc}	26±1^{cd}	21.7±0.4^{ab}	18±3^{a}
	T_m onset (ºC)	150±11^{a}	157±4^{a}	155±13^{a}	160±2^{a}	145±9^{a}	146±10^{a}
	T_m peak (ºC)	180±7^{a}	185.7±0.3^{a}	182±10^{a}	186±1^{a}	183±4^{a}	178±8^{a}
	T_g (ºC)	66±1^{e}	45±3^{a}	59±4^{cd}	64±2de	52±6^{b}	57±5^{bc}

*: onset T_g value and T_m values from the last endotherm

Table 4 shows the results obtained from the DSC analysis, in terms of the glass transition (T_g), melting temperatures (T_m), melting and crystallization enthalpies (ΔH) and percentage of crystallinity (X_c) of PVA-based films deduced from the 1st and 2nd heating scans. ~~In **Figure 6**, only the DSC curves from the 1st heating for the different samples are shown. After erasing the thermal history of the samples, the thermograms obtained in the 2nd heating (not shown) were very similar, exhibiting the glass transition and the melting endotherm, whose enthalpy and onset and peak temperature values are shown in **Table 4**.~~

During the 1st heating, all the thermograms exhibited a glass transition at around 28-55 ºC, typical of semi-crystalline polymers and coherent with that observed by other authors [33]. After the glass transition, multiple crystallization-melting behaviour of ES samples was observed to overlap. This multiple crystallization-melting behaviour reveals that the materials obtained by fast solvent evaporation were mainly in a non-equilibrium glassy state when maintained at temperatures below their T_g [34] and were prone to crystallization during DSC heating to achieve a more thermodynamically stable state [35]. A reduction in PVA crystallinity after the electrospinning process has

also been reported by other authors [34], [36], related to the extremely short solvent evaporation time leading to the formation of highly metastable structures.

In some cases, polymer relaxation, characterized by an endothermic peak at the end of the glass transition, was observed. This relaxation is related with the aging of the glass fraction of the material. The presence of the relaxation endotherm and the overlapped crystallization-melting processes, which disrupt the construction of a realistic integration baseline, hamper the determination of the midpoint of the glass transition temperature in ES samples during the first heating step as well as the integration of the melting endotherm [37]. Due to this, for ES samples, the onset T_g values and the peak temperature of the last endotherm in the 1st heating were only provided in **Table 4**. In the other cases, the midpoint T_g values were shown. The presence of carvacrol decreased the onset (ES samples) and midpoint (cast samples) T_g values of the polymer, to a greater extent than in the samples containing surfactant. This was coherent with the carvacrol plasticizing effect, which was more limited when surfactant entrapped a part of the compound within the micelles.

As concerns the cooling scan and second heating scan, where the sample thermal history was deleted, a multifactorial ANOVA revealed no significant differences in the T_g values from either scan and no significant effect of the processing method, but a significant effect of both the carvacrol and surfactant presence ($p<0.05$). Samples without carvacrol exhibited a mean T_g value of 63 ºC, which decreased to 56 ºC with carvacrol and surfactant and to 48 ºC with only carvacrol, corroborating the plasticizing effects observed from the onset T_g values of the first scan.

By comparing the crystallization (cooling scan) and melting (second heating) temperatures, a supercooling effect was inferred in every case since the T_c values ranged between 142-157 and the T_m between 178-186 ºC. The crystallinity of PVA was obtained from the ΔH_m values (J/g PVA), taking into account the reported ΔH_m value (138.6 J/g PVA) of 100 % crystalline PVA [24]. In cast films, the crystallinity was estimated from the first and second (erased thermal history) heating scans. Neither the presence of carvacrol nor that of surfactant in the first heating was observed to cause any significant differences in these values (of about 40 %); however, under the thermal conditions of the DSC assay (second heating), significant differences in crystallinity were observed between the samples. The crystallinity increased in ES samples when these contained carvacrol (especially when there was no surfactant),

whereas it decreased in cast samples with carvacrol with and without surfactant. This suggests that, after melting, different component interactions were established in the melt that affect the polymer crystallization differently. In the second heating step, the crystallinity of PVA ranged between 18-30 % concurring with the values obtained by other authors [24], and was lower than that reached during the casting process determined in the first heating scan.

Therefore, a practically amorphous structure can be assumed for the ES samples, which tend to crystallize at temperatures above the T_g value, whereas cast samples exhibited a structure that was highly crystalline in nature (nearly 40 %), as was also deduced from the thermal degradation behaviour of the different samples.

4. Conclusions

PVA aqueous solutions (15 % w/w) containing CA (15 g/100 g polymer) exhibited good electrospinning behaviour, leading to loaded matts with fibres and spherical beds, that retained up to 83 % of the active, giving rise to matrices with up to 12 g carvacrol/100 g polymer. The greatest encapsulation efficiency occurred in the blend without surfactant (83 %) and the formulations with surfactant exhibited similar encapsulation efficiency to that obtained in the casting process (75-77 %). Two fractions of carvacrol could be distinguished in the encapsulating materials; the more strongly bonded, non-thermo-releasable fraction was higher (40 % of the total) in ES samples without surfactant and lower in those containing surfactant, whereas in cast samples this fraction accounted for about 18 % of total carvacrol. Therefore, the addition of the Tween 85 surfactant limited the retention of CA by the PVA matrix, due to its less stable micelle-encapsulating effect that reduced the amount of carvacrol that was more strongly bonded to the polymer. PVA-CA interactions also promoted the plasticization of the polymer, which was practically amorphous in the ES samples and semi-crystalline (about 40 % crystallinity) in the cast samples. Thus, the use of electrospinning as a delivery system for the purposes of successfully applying carvacrol-loaded PVA fibres in active packaging materials represents an interesting strategy, while the PVA layer would provide oxygen barrier capacity coherent with its polar nature.

5. Acknowledgements

The authors thank the Ministerio de Economia y Competitividad (MINECO) of Spain, for the financial support provided for this study as part of the project AGL2016-76699-R. The author A. Tampau also thanks MINECO for the pre-doctoral research grant #BES-2014-068100.

6. Data availability

The raw/processed data required to reproduce these findings cannot be shared at this time due to legal or ethical reasons.

7. Bibliography

[1] L. Sánchez-González, M. Vargas, C. González-Martínez, A. Chiralt, M. Cháfer, Characterization of edible films based on hydroxypropylmethylcellulose and tea tree essential oil, Food Hydrocoll. 23 (2009) 2102–2109. doi:10.1016/j.foodhyd.2009.05.006.

[2] R. Shemesh, M. Krepker, D. Goldman, Y. Danin-Poleg, Y. Kashi, N. Nitzan, A. Vaxman, E. Segal, Antibacterial and antifungal LDPE films for active packaging, Polym. Adv. Technol. 26 (2015) 110–116. doi:10.1002/pat.3434.

[3] A. González, C.I. Alvarez Igarzabal, Soy protein – Poly (lactic acid) bilayer films as biodegradable material for active food packaging, Food Hydrocoll. 33 (2013) 289–296. doi:10.1016/j.foodhyd.2013.03.010.

[4] C.C. Thong, D.C.L. Teo, C.K. Ng, Application of polyvinyl alcohol (PVA) in cement-based composite materials: A review of its engineering properties and microstructure behavior, Constr. Build. Mater. 107 (2016) 172–180. doi:10.1016/j.conbuildmat.2015.12.188.

[5] Y. Di, J. Li, T. Ye, Y. Xiaoyun, The preparation and mechanical properties of novel PVA/SiO 2 film, J. Exp. Nanosci. 10 (2015) 1137–1142. doi:10.1080/17458080.2014.980447.

[6] A. Ultee, L.G.M. Gorris, E.J. Smid, Bactericidal activity of carvacrol towards the food-borne pathogen Bacillus cereus, J. Appl. Microbiol. 85 (1998) 211–218. doi:10.1046/j.1365-2672.1998.00467.x.

562 [7] A. Ben Arfa, S. Combes, L. Preziosi-Belloy, N. Gontard, P. Chalier, Antimicrobial
563 activity of carvacrol related to its chemical structure, Lett. Appl. Microbiol. 43
564 (2006) 149–154. doi:10.1111/j.1472-765X.2006.01938.x.

565 [8] S. Tunc, E. Chollet, P. Chalier, L. Preziosi-Belloy, N. Gontard, Combined effect of
566 volatile antimicrobial agents on the growth of Penicillium notatum, Int. J. Food
567 Microbiol. 113 (2007) 263–270. doi:10.1016/j.ijfoodmicro.2006.07.004.

568 [9] S. Burt, Essential oils: Their antibacterial properties and potential applications in
569 foods – A review, Int. J. Food Microbiol. 94 (2004) 223–253.
570 doi:10.1016/j.ijfoodmicro.2004.03.022.

571 [10] Z.E. Suntres, J. Coccimiglio, M. Alipour, The Bioactivity and Toxicological Actions
572 of Carvacrol, Crit. Rev. Food Sci. Nutr. 55 (2015) 304–318.
573 doi:10.1080/10408398.2011.653458.

574 [11] M.A. López-Mata, S. Ruiz-Cruz, N.P. Silva-Beltrán, J.D.J. Ornelas-Paz, P.B.
575 Zamudio-Flores, S.E. Burruel-Ibarra, Physicochemical, antimicrobial and
576 antioxidant properties of chitosan films incorporated with carvacrol, Molecules. 18
577 (2013) 13735–13753. doi:10.3390/molecules181113735.

578 [12] L. Atarés, A. Chiralt, Essential oils as additives in biodegradable films and coatings
579 for active food packaging, Trends Food Sci. Technol. 48 (2016) 51–62.
580 doi:10.1016/j.tifs.2015.12.001.

581 [13] P. Wen, D.-H.H. Zhu, H. Wu, M.-H.H. Zong, Y.-R.R. Jing, S.-Y.Y. Han,
582 Encapsulation of cinnamon essential oil in electrospun nanofibrous film for active
583 food packaging, Food Control. 59 (2016) 366–376.
584 doi:10.1016/j.foodcont.2015.06.005.

585 [14] S. Torres-Giner, Multifunctional and Nanoreinforced Polymers for Food
586 Packaging, Multifunct. Nanoreinforced Polym. Food Packag. (2011) 108–125.
587 doi:10.1533/9780857092786.1.108.

588 [15] B. Ghorani, N. Tucker, Fundamentals of electrospinning as a novel delivery
589 vehicle for bioactive compounds in food nanotechnology, Food Hydrocoll. 51
590 (2015) 227–240. doi:10.1016/j.foodhyd.2015.05.024.

[16] A. Tampau, C. González-Martinez, A. Chiralt, Carvacrol encapsulation in starch or PCL based matrices by electrospinning, J. Food Eng. 214 (2017) 245–256. doi:10.1016/j.jfoodeng.2017.07.005.

[17] L. Quiles-Carrillo, N. Montanes, J.M. Lagaron, R. Balart, S. Torres-Giner, Bioactive multilayer polylactide films with controlled release capacity of gallic acid accomplished by incorporating electrospun nanostructured coatings and interlayers, Appl. Sci. 9 (2019) 533. doi:10.3390/app9030533.

[18] J.L. Castro-Mayorga, M.J. Fabra, L. Cabedo, J.M. Lagaron, On the use of the electrospinning coating technique to produce antimicrobial polyhydroxyalkanoate materials containing in situ-stabilized silver nanoparticles, Nanomaterials. 7 (2017). doi:10.3390/nano7010004.

[19] K. Figueroa-Lopez, J. Castro-Mayorga, M. Andrade-Mahecha, L. Cabedo, J. Lagaron, Antibacterial and Barrier Properties of Gelatin Coated by Electrospun Polycaprolactone Ultrathin Fibers Containing Black Pepper Oleoresin of Interest in Active Food Biopackaging Applications, Nanomaterials. 8 (2018) 199. doi:10.3390/nano8040199.

[20] J. Tao, Effects of Molecular Weight and Solution Concentration on Electrospinning of PVA, Master Thesis, Mater. Sci. Eng. Worcester Polytech. Inst. (2003) 1–107. https://digitalcommons.wpi.edu/etd-theses/889.

[21] S.P. Rwei, C.C. Huang, Electrospinning PVA solution-rheology and morphology analyses, Fibers Polym. 13 (2012) 44–50. doi:10.1007/s12221-012-0044-9.

[22] R.K. Owusu Apenten, Q.-H. Zhu, Interfacial parameters for selected Spans and Tweens at the hydrocarbon—water interface, Food Hydrocoll. 10 (1996) 27–30. doi:10.1016/S0268-005X(96)80050-6.

[23] A. Sze, D. Erickson, L. Ren, D. Li, Zeta-potential measurement using the Smoluchowski equation and the slope of the current-time relationship in electroosmotic flow, J. Colloid Interface Sci. 261 (2003) 402–410. doi:10.1016/S0021-9797(03)00142-5.

[24] M. Hdidar, S. Chouikhi, A. Fattoum, M. Arous, Effect of hydrolysis degree and mass molecular weight on the structure and properties of PVA films, Ionics (Kiel). 23 (2017) 3125–3135. doi:10.1007/s11581-017-2103-0.

[25] M. Wiśniewska, V. Bogatyrov, I. Ostolska, K. Szewczuk-Karpisz, K. Terpiłowski, A. Nosal-Wiercińska, Impact of poly(vinyl alcohol) adsorption on the surface characteristics of mixed oxide MnxOy–SiO2, Adsorption. 22 (2016) 417–423. doi:10.1007/s10450-015-9696-2.

[26] A. Bhattacharya, P. Ray, Studies on surface tension of poly (vinyl alcohol): Effect of concentration, temperature, and addition of chaotropic agents, J. Appl. Polym. Sci. 93 (2004) 122–130. doi:10.1002/app.20436.

[27] A. Koski, K. Yim, S. Shivkumar, Effect of molecular weight on fibrous PVA produced by electrospinning, Mater. Lett. 58 (2004) 493–497. doi:10.1016/S0167-577X(03)00532-9.

[28] Á. Perdones, A. Chiralt, M. Vargas, Properties of film-forming dispersions and films based on chitosan containing basil or thyme essential oil, Food Hydrocoll. 57 (2016) 271–279. doi:10.1016/j.foodhyd.2016.02.006.

[29] A. Cano, E. Fortunati, M. Cháfer, J.M. Kenny, A. Chiralt, C. González-Martínez, Properties and ageing behaviour of pea starch films as affected by blend with poly(vinyl alcohol), Food Hydrocoll. 48 (2015) 84–93. doi:10.1016/j.foodhyd.2015.01.008.

[30] S. Farah, D.G. Anderson, R. Langer, Physical and mechanical properties of PLA, and their functions in widespread applications — A comprehensive review, Adv. Drug Deliv. Rev. 107 (2016) 367–392. doi:10.1016/j.addr.2016.06.012.

[31] R. Inai, M. Kotaki, S. Ramakrishna, Structure and properties of electrospun PLLA single nanofibres, Nanotechnology. 16 (2005) 208–213. doi:10.1088/0957-4484/16/2/005.

[32] E.K. Kostakova, L. Meszaros, G. Maskova, L. Blazkova, T. Turcsan, D. Lukas, Crystallinity of Electrospun and Centrifugal Spun Polycaprolactone Fibers: A Comparative Study, J. Nanomater. 2017 (2017). doi:10.1155/2017/8952390.

[33] I. Restrepo, C. Medina, V. Meruane, A. Akbari-Fakhrabadi, P. Flores, S. Rodríguez-Llamazares, The effect of molecular weight and hydrolysis degree of poly(vinyl alcohol)(PVA) on the thermal and mechanical properties of poly(lactic acid)/PVA blends, Polimeros. 28 (2018) 169–177. doi:10.1590/0104-1428.03117.

[34] M.J. Parker, Test Methods for Physical Properties, in: A. Kelly, C.B.T.-C.C.M. Zweben (Eds.), Compr. Compos. Mater., Elsevier, Oxford, 2000: pp. 183–226. doi:10.1016/B0-08-042993-9/00074-7.

[35] B.B. Sauer, W.G. Kampert, E. Neal Blanchard, S.A. Threefoot, B.S. Hsiao, Temperature modulated DSC studies of melting and recrystallization in polymers exhibiting multiple endotherms, Polymer (Guildf). 41 (2000) 1099–1108. doi:10.1016/S0032-3861(99)00258-X.

[36] M.S. Enayati, T. Behzad, P. Sajkiewicz, R. Bagheri, L. Ghasemi-Mobarakeh, W. Łojkowski, Z. Pahlevanneshan, M. Ahmadi, Crystallinity study of electrospun poly (vinyl alcohol) nanofibers: effect of electrospinning, filler incorporation, and heat treatment, Iran. Polym. J. (English Ed. 25 (2016) 647–659. doi:10.1007/s13726-016-0455-3.

[37] C.A. Avila-Orta, F.J. Medellín-Rodríguez, M. V. Dávila-Rodríguez, Y.A. Aguirre-Figueroa, K. Yoon, B.S. Hsiao, Morphological features and melting behavior of nanocomposites based on isotactic polypropylene and multiwalled carbon nanotubes, J. Appl. Polym. Sci. 106 (2007) 2640–2647. doi:10.1002/app.26823.